Neutrino mass matrices with M_{ee}=0

Yoni BenTov and A. Zee

Neutrino Mass Matrices with $M_{ee} = 0$

Yoni BenTov[1] and A. Zee[1,2]

[1] Department of Physics, University of California, Santa Barbara CA 93106
[2] Kavli Institute for Theoretical Physics, University of California, Santa Barbara CA 93106

Abstract

Motivated by the possibility that the amplitude for neutrinoless double beta decay may be much smaller than the planned sensitivity of future experiments, we study ansatze for the neutrino mass matrix with $M_{ee} = 0$. For the case in which CP is conserved, we consider two classes of real-valued mass matrices: "Class I" defined by $|M_{e\mu}| = |M_{e\tau}|$, and "Class II" defined by $|M_{\mu\mu}| = |M_{\tau\tau}|$. The important phenomenological distinction between the two is that Class I permits only "small" values of V_{e3} up to ~ 0.03, while Class II admits "large" values of V_{e3} up to its empirical upper limit of 0.22. Then we introduce CP-violating complex phases into the mass matrix. We show that it is possible to have tribimaximal mixing with $M_{ee} = 0$ and $|M_{\mu\tau}| = |M_{\mu\mu}| = |M_{\tau\tau}|$ if the Majorana phase angles are $\pm\pi/4$. Alternatively, for smaller values of $|M_{\mu\tau}| = |M_{\mu\mu}| = |M_{\tau\tau}|$ it is possible to obtain $|V_{e3}| \sim 0.2$ and generate relatively large CP-violating amplitudes. To eliminate phase redundancy, we emphasize rephasing any mass matrix with $M_{ee} = 0$ into a standard form with two complex phases. The discussion alternates between analytical and numerical but remains purely phenomenological, without any attempt to derive mass matrices from a fundamental theory.

1 Data and Conventions

The present empirical knowledge of neutrino oscillations can be summarized qualitatively as follows [1, 2]. We observe a deficiency of electron neutrinos originating from the sun and attribute this to oscillations described roughly by a mixing angle $\theta_{\text{solar}} \sim 0.5 - 0.8$ and a mass-squared difference $\Delta m^2_{\text{solar}} \sim 10^{-5} - 10^{-4}$ eV^2. We also observe a deficiency of muon neutrinos in the earth's atmosphere from incident cosmic rays and attribute this to oscillations described roughly by a mixing angle $\theta_{\text{atm}} \sim 0.6 - 1$ and a mass-squared difference $\Delta m^2_{\text{atm}} \sim 10^{-3}$ eV^2. The commonly accepted theoretical interpretation of the data is that all three flavors of neutrinos – ν_e, ν_μ and ν_τ – participate in oscillations. In this work we base our quantitative empirical understanding of three-flavor neutrino oscillations on the analysis of Gonzalez-Garcia and Maltoni [2], who report the entries of the 3-by-3 neutrino mixing matrix V as having magnitudes[1]

$$|V_{\text{exp}}| \approx \begin{pmatrix} 0.77\text{–}0.86 & 0.50\text{–}0.63 & 0.00\text{–}0.22 \\ 0.22\text{–}0.56 & 0.44\text{–}0.73 & 0.57\text{–}0.80 \\ 0.21\text{–}0.55 & 0.40\text{–}0.71 & 0.59\text{–}0.82 \end{pmatrix} \ , \tag{1.1}$$

---

[1]There are varying degrees of confidence levels assigned to the different fits in the review. To impose as little theoretical prejudice as possible, we will always quote the 3σ bounds, which are the least restrictive.

where the bounds are correlated such that V is unitary. We also quote the recently updated report by Gonzalez-Garcia, Maltoni and Salvado [3] for the angles[2]

$$0.620 \leq \theta_1 \leq 0.934 , \quad 0.00 \leq \theta_2 \leq 0.218 , \quad 0.550 \leq \theta_3 \leq 0.658$$

and the mass-squared differences

$$m_2^2 - m_1^2 = 7.59 \begin{pmatrix} +0.61 \\ -0.69 \end{pmatrix} \times 10^{-5} \text{ eV}^2 , \quad \text{and}$$

$$m_3^2 - m_1^2 = \begin{cases} +2.46 \pm 0.37 \times 10^{-3} \text{ eV}^2 & (\text{``normal hierarchy''}) \\ -2.36 \pm 0.37 \times 10^{-3} \text{ eV}^2 & (\text{``inverted hierarchy''}) \end{cases} .$$

Although we know the mass-squared differences $m_{ij}^2 \equiv m_i^2 - m_j^2$, we do not know the actual value of any of the m_i. Thus to compare with oscillation data, we compute the ratio of mass-squared differences

$$R \equiv \frac{m_3^2 - m_1^2}{m_2^2 - m_1^2} = \begin{cases} +25.5 \text{ to } +41.0 & (\text{``normal'' hierarchy}) \\ -39.6 \text{ to } -24.3 & (\text{``inverted'' hierarchy}) \end{cases} . \tag{1.2}$$

To study the mixing matrix, we use the standard angular parameterization [4] for unitary matrices given by

$$V = \mathcal{K} V_{\text{PMNS}} \mathcal{M} , \quad \text{where} \quad \mathcal{K} \equiv \text{diag}(e^{i\kappa_1}, e^{i\kappa_2}, e^{i\kappa_3}) , \quad \mathcal{M} \equiv \text{diag}(e^{i\rho}, e^{i\sigma}, 1) \tag{1.3}$$

and

$$\begin{aligned}
V_{\text{PMNS}} &\equiv \begin{pmatrix} 1 & 0 & 0 \\ 0 & c_1 & s_1 \\ 0 & s_1 & -c_1 \end{pmatrix} \begin{pmatrix} c_2 & 0 & \hat{s}_2^* \\ 0 & 1 & 0 \\ -\hat{s}_2 & 0 & c_2 \end{pmatrix} \begin{pmatrix} -c_3 & s_3 & 0 \\ s_3 & c_3 & 0 \\ 0 & 0 & 1 \end{pmatrix} \\
&= \begin{pmatrix} -c_2 c_3 & c_2 s_3 & \hat{s}_2^* \\ c_1 s_3 + s_1 \hat{s}_2 c_3 & c_1 c_3 - s_1 \hat{s}_2 s_3 & s_1 c_2 \\ s_1 s_3 - c_1 \hat{s}_2 c_3 & s_1 c_3 + c_1 \hat{s}_2 s_3 & -c_1 c_2 \end{pmatrix} .
\end{aligned} \tag{1.4}$$

Here $c_I \equiv \cos\theta_I$, $s_I \equiv \sin\theta_I$ and $\hat{s}_2 \equiv s_2 e^{i\delta_{\text{CP}}}$, and we have chosen the sign conventions in V_{PMNS} to minimize the number of minus signs that appear. The angles in $\mathcal{K}$ are unphysical and can be chosen arbitrarily.

We will assume that the neutrinos are Majorana. In this case the Majorana phase matrix $\mathcal{M}$ is physically meaningful and contributes to the amplitude for neutrinoless double beta decay. In addition, the neutrino mass matrix M is symmetric. We will work in the basis for which the charged lepton mass matrix is diagonal with real positive entries, called the flavor basis. In this basis the neutrino mass matrix is

$$M = V^* D V^\dagger \tag{1.5}$$

---

[2]The report quotes two sets of ranges for the angles, depending on uncertainties in the capture cross section of gallium. The distinction between the two sets is a slight change in the range of θ_3 and in the upper bound of θ_2, with θ_1 and the mass-squared splittings unaffected. We take the least restrictive bounds whenever possible. Also, the notation in the reference is $\theta_{23} \equiv \theta_1$, $\theta_{13} \equiv \theta_2$ and $\theta_{12} \equiv \theta_3$.

where $D \equiv \mathrm{diag}(m_1, m_2, m_3)$. Here $m_i \geq 0$ denote the physical masses of the three neutrinos.

There is some degree of rephasing freedom in the neutrino mass matrix M, and we will return to this point in a later section on CP violation. For now we simply wish to clarify a potential source of confusion for the case in which CP is conserved. If CP is conserved, then M can be taken as real, and we can without loss of generality set $\delta_{\mathrm{CP}} = 0$. However, we cannot set ρ and σ equal to zero, since the Majorana phase matrix $\mathcal{M}$ appears squared in the mass matrix M. With $\mathcal{K} = I$ and $\delta_{\mathrm{CP}} = 0$, we have $M = \mathcal{K}^* V_{\mathrm{PMNS}}^* \mathcal{M}^* D \mathcal{M}^* V_{\mathrm{PMNS}}^\dagger \mathcal{K}^* = V_{\mathrm{PMNS}} \tilde{D} \, V_{\mathrm{PMNS}}^T$, where we have defined the diagonal matrix

$$\tilde{D} \equiv \begin{pmatrix} \tilde{m}_1 & & \\ & \tilde{m}_2 & \\ & & m_3 \end{pmatrix} \quad \text{with } \tilde{m}_1 \equiv m_1 \, e^{-i2\rho} \text{ and } \tilde{m}_2 \equiv m_2 \, e^{-i2\sigma} \, . \tag{1.6}$$

The notation is such that $m_{1,2}$ are real and positive while $\tilde{m}_{1,2}$ are complex. (Also, with our phase conventions m_3 is always real and positive.) Thus the choice of 0 or $\frac{\pi}{2}$ for ρ and σ generates non-removable minus signs associated with m_1 and m_2, which yield qualitatively different textures for the mass matrix M. In the CP-conserving case, it is convenient to separate these signs from V and instead associate them with the diagonal matrix $\tilde{D}$.

2   Neutrinoless Double Beta Decay and $M_{ee} = 0$

As discussed at the end of the previous section, the choice of signs in $\tilde{m}_{1,2}$ imply qualitatively different textures for the mass matrix. To motivate a particular choice, we recall the well-known fact that a direct way to measure one of the entries in M is in neutrinoless double beta decay, the amplitude of which is proportional to $|M_{ee}|$. From Eqs. (1.3-1.5) we have

$$|M_{ee}| = \left| c_2^2 \left(c_3^2 \, e^{i\alpha_1} m_1 + s_3^2 \, e^{i\alpha_2} m_2 \right) + s_2^2 m_3 \right| \tag{2.1}$$

where $\alpha_1 \equiv -2(\rho + \delta_{\mathrm{CP}})$ and $\alpha_2 \equiv -2(\sigma + \delta_{\mathrm{CP}})$. Thus in general, $|M_{ee}|$ depends on all three masses m_1, m_2 and m_3, the two angles θ_2 and θ_3, and two phases α_1 and α_2.

A brief review of the current status of neutrinoless double beta decay was given recently by Bilenky [5], which we now summarize[3]. The Heidelberg-Moscow and CUORICINO experiments imply the upper bounds $|M_{ee}| \leq (0.3-1.2)$ eV and $|M_{ee}| \leq (0.3-1.7)$ eV, respectively. The future experiments CUORE, EXO, GENIUS and MAJORANA plan to significantly improve the sensitivity to roughly $|M_{ee}| \sim (1-7) \times 10^{-2}$ eV.

These values should be understood in comparison to the m_{ij}^2 data above Eq. (1.2), which imply

$$8.3 \times 10^{-3} \mathrm{eV} \leq \sqrt{m_{21}^2} \leq 9.1 \times 10^{-3} \mathrm{eV} \text{ and } 4.6 \times 10^{-2} \mathrm{eV} \leq \sqrt{m_{31}^2} \leq 5.3 \times 10^{-2} \mathrm{eV}$$

for the normal hierarchy $m_1 < m_2 < m_3$.

---

[3]An early review of neutrinoless double beta decay was given by Zel'dovich and Klhopov [6].

If $m_3 \gg m_{1,2}$, then $m_3 \approx \sqrt{m_{31}^2} \sim 5 \times 10^{-2}$ eV, but since $s_2^2 \leq 4.68 \times 10^{-2}$ the large m_3 is suppressed by the small s_2^2 in $|M_{ee}|$. Thus $|M_{ee}|$ is at most $\sim 10^{-3}$ eV, which is an order of magnitude smaller than the planned sensitivity of future experiments. If $m_3 > m_{1,2}$ but all three masses are still almost equal, then the m_3 term drops out and $|M_{ee}| \approx m_1 c_2^2 |c_3^2 + s_3^2 e^{i(\alpha_2 - \alpha_1)}|$. With the bounds given below Eq. (1.1), this implies $0.26 \leq |M_{ee}|/m_1 \leq 1$, where the upper bound occurs for $\alpha_2 = \alpha_1$ and $\theta_2 = 0$.

Thus for any normal hierarchy, $|M_{ee}|$ tends to be smaller than the other entries in M. Using this as guidance, we suppose that M_{ee} could be tiny and thereby set $M_{ee} = 0$. In other words, throughout this paper we assume that the amplitude for neutrinoless double beta decay is zero, at least as a leading order approximation [7, 8, 9, 10].

3   Tribimaximal Mixing with $M_{ee} = 0$

As has been noted independently by many authors [11, 12], the theoretical ansatz of "tribimaximal mixing" defined as

$$V_{\text{PMNS}} = V_{\text{TB}} \equiv \begin{pmatrix} \frac{-2}{\sqrt{6}} & \frac{1}{\sqrt{3}} & 0 \\ \frac{1}{\sqrt{6}} & \frac{1}{\sqrt{3}} & \frac{1}{\sqrt{2}} \\ \frac{1}{\sqrt{6}} & \frac{1}{\sqrt{3}} & \frac{-1}{\sqrt{2}} \end{pmatrix} \approx \begin{pmatrix} -0.82 & 0.58 & 0 \\ 0.41 & 0.58 & 0.71 \\ 0.41 & 0.58 & -0.71 \end{pmatrix} \tag{3.1}$$

is compatible with the empirical bounds given in $|V_{\text{exp}}|$. If neutrino oscillations conserve CP, then we can write the neutrino mass matrix in the flavor basis as $M = V_{\text{PMNS}} \tilde{D} V_{\text{PMNS}}^T$, where $\tilde{D} \equiv \text{diag}(\tilde{m}_1, \tilde{m}_2, m_3)$ and $\tilde{m}_i \equiv \pm m_i$ with uncorrelated signs. We can thereby define a "tribimaximal mass matrix" $M_{\text{TB}} \equiv V_{\text{TB}} \tilde{D} V_{\text{TB}}^T$ associated with the ansatz of tribimaximal mixing. Explicitly, this mass matrix reads[4]

$$M_{\text{TB}} = \frac{1}{3} \left[\tilde{m}_1 \begin{pmatrix} 2 & -1 & -1 \\ & 1/2 & 1/2 \\ & & 1/2 \end{pmatrix} + \tilde{m}_2 \begin{pmatrix} 1 & 1 & 1 \\ & 1 & 1 \\ & & 1 \end{pmatrix} \right] + \frac{m_3}{2} \begin{pmatrix} 0 & 0 & 0 \\ & 1 & -1 \\ & & 1 \end{pmatrix} . \tag{3.2}$$

For all values of $\tilde{m}_i$ and m_3, this matrix exhibits the symmetry $M_{e\mu} = M_{e\tau}$ and $M_{\mu\mu} = M_{\tau\tau}$ [13, 17]. We stress that although the condition $V = V_{\text{TB}}$ necessarily implies $M_{e\mu} = M_{e\tau}$ and $M_{\mu\mu} = M_{\tau\tau}$, the converse is not true: $M_{e\mu} = M_{e\tau}$ and $M_{\mu\mu} = M_{\tau\tau}$ do not necessarily imply tribimaximal mixing.

Two appealing examples of tribimaximal mass matrices with $M_{ee} = 0$ are obtained by choosing the values $(\tilde{m}_1, \tilde{m}_2, m_3) = (-1, 2, 9)$ and $(-1, 2, 11)$, which give

$$M_{\text{TB}}^{(-1,+2,9)} = m_\nu \begin{pmatrix} 0 & 1 & 1 \\ & 5 & -4 \\ & & 5 \end{pmatrix} \quad \text{and} \quad M_{\text{TB}}^{(-1,+2,11)} = m_\nu \begin{pmatrix} 0 & 1 & 1 \\ & 6 & -5 \\ & & 6 \end{pmatrix} \tag{3.3}$$

respectively. The first has $R \approx 27$, while the second has $R = 40$ exactly, which correspond nearly to the lower and upper empirical bounds for R.

---

[4]Since the mass matrix is symmetric, we display explicitly only its upper triangle.

In the mass matrix M_{TB} the sign flip $(\tilde{m}_1, \tilde{m}_2) \to (-\tilde{m}_1, -\tilde{m}_2)$ effects the exchange

$$(M_{\mu\mu}, M_{\mu\tau}) \to -(M_{\mu\tau}, M_{\mu\mu}) \, . \tag{3.4}$$

This means that given one tribimaximal mass matrix, we can always find a second tribimaximal mass matrix by interchanging the magnitudes of $M_{\mu\mu}$ and $M_{\mu\tau}$.

Thus from (3.3) we can immediately write the matrices[5]

$$M_{\mathrm{TB}}^{(+1,-2,9)} = m_\nu \begin{pmatrix} 0 & 1 & 1 \\ & 4 & -5 \\ & & 4 \end{pmatrix} \quad \text{and} \quad M_{\mathrm{TB}}^{(+1,-2,11)} = m_\nu \begin{pmatrix} 0 & 1 & 1 \\ & 5 & -6 \\ & & 5 \end{pmatrix} \tag{3.5}$$

which also predict $R \approx 27$ and $R = 40$ respectively.

A mass matrix that resembles the examples given above but with non-tribimaximal mixing is[6]

$$M_{\mathrm{nTB}} \equiv m_\nu \begin{pmatrix} \frac{1}{5} & 1 & 1 \\ & 5 & -5 \\ & & 3 \end{pmatrix} \implies R \approx 29 \quad \text{and} \quad |V_{\mathrm{PMNS}}| \approx \begin{pmatrix} 0.84 & 0.54 & 0.02 \\ 0.33 & 0.54 & 0.77 \\ 0.43 & 0.65 & 0.63 \end{pmatrix} \tag{3.6}$$

which was suggested in the context of a particular model [15]. Since $M_{\mu\mu} \neq M_{\tau\tau}$ the resulting mixing matrix is not tribimaximal, as can be seen from the nonzero V_{e3}. On the other hand, both M_{nTB} and M_{TB} share the property $M_{e\mu} = M_{e\tau}$. The matrix M_{nTB} also has M_{ee} smaller than the other entries.

Motivated by this discussion,[7] we consider the "Class I" ansatz

$$M_{\mathrm{I}} \equiv m_\nu \begin{pmatrix} 0 & 1 & 1 \\ & M_{\mu\mu} & M_{\mu\tau} \\ & & M_{\tau\tau} \end{pmatrix} \qquad \text{(Class I)} \tag{3.7}$$

with $M_{ee} = 0$ and $M_{e\mu} = M_{e\tau}$, and the "Class II" ansatz[8]

$$M_{\mathrm{II}} \equiv m_\nu \begin{pmatrix} 0 & M_{e\mu} & M_{e\tau} \\ & 5 & M_{\mu\tau} \\ & & 5 \end{pmatrix} \qquad \text{(Class II)} \tag{3.8}$$

---

[5]We have used the rephasing freedom in M to move around the minus signs. See Section 4.

[6]Many authors have proposed parametrizations of deviations from tribimaximal mixing [14].

[7]We do not intend to classify the most general deviations from tribimaximal mixing or from $\mu\tau$-symmetry. We simply propose a set of $M_{ee} = 0$ textures for the mass matrix and study under which circumstances they can fit data.

[8]In Class II, the value $M_{\mu\mu} = M_{\tau\tau} = 5$ is merely a convenient normalization for comparing the empirically allowed mass matrices with those of Class I.

with $M_{\mu\mu} = M_{\tau\tau}$. Since oscillation experiments cannot determine the overall scale of M, we from now on set $m_\nu = 1$ and treat the entries of M as dimensionless numbers.

We also remind the reader that throughout this paper we work in the flavor basis, in which the mass matrix for the charged leptons is diagonal.

Finally, we emphasize that we make no attempt to derive these mass matrices from any theoretical model but instead study these matrices on purely phenomenological grounds.[9]

4 Rephasing the Mass Matrix

Before proceeding to study the matrices M_{I} and M_{II}, we should comment on the significance of various signs that may appear in the mass matrix. Consider the most general 3-by-3 complex symmetric matrix M with $M_{ee} = 0$:

$$
M = \begin{pmatrix} 0 & a_{e\mu}\, e^{i\varphi_{e\mu}} & a_{e\tau}\, e^{i\varphi_{e\tau}} \\ & a_{\mu\mu}\, e^{i\varphi_{\mu\mu}} & a_{\mu\tau}\, e^{i\varphi_{\mu\tau}} \\ & & a_{\tau\tau}\, e^{i\varphi_{\tau\tau}} \end{pmatrix} \tag{4.1}
$$

where $a_{\alpha\beta}$ and $\varphi_{\alpha\beta}$ are real numbers. Using the form $M = V^* D V^\dagger$ with $V = \mathcal{K} V_{\mathrm{PMNS}} \mathcal{M}$ introduced in Section 1, we have $M = \mathcal{K}^* \hat{M} \mathcal{K}^*$, where $\hat{M} = V_{\mathrm{PMNS}}^* \mathcal{M}^* D \mathcal{M}^* V_{\mathrm{PMNS}}^\dagger$, and thus $\hat{M} = \mathcal{K} M \mathcal{K}$. We are free to choose the phases in $\mathcal{K}$ as we please, since they are unphysical. Choosing $\kappa_1 = \frac{1}{2}\varphi_{\mu\mu} - \varphi_{e\mu}$, $\kappa_2 = -\frac{1}{2}\varphi_{\mu\mu}$ and $\kappa_3 = -\frac{1}{2}\varphi_{\tau\tau}$ gives

$$
\hat{M} = \begin{pmatrix} 0 & a_{e\mu} & a_{e\tau}\, e^{i\varphi} \\ & a_{\mu\mu} & a_{\mu\tau}\, e^{i\eta} \\ & & a_{\tau\tau} \end{pmatrix} \tag{4.2}
$$

where $\varphi \equiv \varphi_{e\tau} - \varphi_{e\mu} + \frac{1}{2}\varphi_{\mu\mu} - \frac{1}{2}\varphi_{\tau\tau}$ and $\eta \equiv \varphi_{\mu\tau} - \frac{1}{2}\varphi_{\mu\mu} - \frac{1}{2}\varphi_{\tau\tau}$. We may thus dispense with the matrix M and consider only the matrix $\hat{M}$. Henceforth when there is no risk of confusion we put any mass matrix M into the form of $\hat{M}$ and then drop the hat for notational convenience.

For the case in which M is real, the phases reduce to the signs ± 1. The above argument shows that any real-valued neutrino mass matrix with $M_{ee} = 0$ can be put into the form

$$
M = \begin{pmatrix} 0 & |M_{e\mu}| & \zeta|M_{e\tau}| \\ & |M_{\mu\mu}| & \zeta'|M_{\mu\tau}| \\ & & |M_{\tau\tau}| \end{pmatrix} \tag{4.3}
$$

where each of ζ and ζ' can be either $+1$ or -1. The matrix M can be multiplied on both sides by the matrix $Z \equiv \mathrm{diag}(1, 1, -1)$, which transforms $(\zeta, \zeta') \to (-\zeta, -\zeta')$ and thereby leaves the product $\zeta\zeta'$ unchanged. Since $\det(ZMZ) = \det M$, all observables based on the M in (4.3) are invariant under $M \to ZMZ$ and therefore depend only on $\mathrm{sgn}(M_{e\tau}M_{\mu\tau})$, not

---

[9]For example, it may be possible to derive such one-zero textures from group theory, but such an investigation is beyond the scope of this work.

on $\zeta = \mathrm{sgn}(M_{e\tau})$ and $\zeta' = \mathrm{sgn}(M_{\mu\tau})$ individually.

If we allow $M_{\mu\tau}$ to range over all real numbers, then in both Classes I and II we can take all other entries in M to be strictly non-negative. Given this choice, it will turn out furthermore that only $M_{\mu\tau} < 0$ can fit data. This can be seen from the form of M_{tribi} with $m_3 \gg m_{1,2}$.

To summarize, we will first study real-valued mass matrices of Classes I and II given in Eqs. (3.7) and (3.8) with $M_{ee} = 0$, $M_{\mu\tau} < 0$ and all other entries positive.

5 Analytic Preliminaries

If CP is conserved in the neutrino sector, there are 6 potential observables in neutrino phenomenology: 3 angles θ_i and 3 masses m_i. Accordingly, a general 3-by-3 real symmetric matrix has 6 independent parameters and thereby makes no predictions. By fixing $M_{ee} = 0$ we impose a constraint and thus fix one of the parameters [15], namely the angle θ_2 (and thus V_{e3}), according to the relation

$$\tan^2 \theta_2 = - \left(\frac{c_3^2 \tilde{m}_1 + s_3^2 \tilde{m}_2}{m_3} \right) . \tag{5.1}$$

Empirically we know that $\theta_2 \leq 0.22$, so $\tan^2 \theta_2 \ll 1$. This tells us that we cannot have $m_3 \ll m_1 \sim m_2$, thus forbidding the inverted hierarchy[10] for the ansatz $M_{ee} = 0$ [16].

As a limiting case, for $\theta_2 \to 0$ we predict $m_1 \to m_2 \tan^2 \theta_3$ and thus fix all three neutrino masses. Since $0.36 \leq \tan^2 \theta_3 \leq 0.60$ and $6.9 \times 10^{-5}\,\mathrm{eV}^2 \leq m_2^2 - m_1^2 \leq 8.2 \times 10^{-5}\,\mathrm{eV}^2$, we have

$$\lim_{\theta_2 \to 0} m_1 = \sqrt{\frac{m_2^2 - m_1^2}{\cot^4 \theta_3 - 1}} = 6.4 \times 10^{-3}\,\mathrm{eV} \ \ \text{to} \ \ 1.1 \times 10^{-2}\,\mathrm{eV}$$

and

$$\lim_{\theta_2 \to 0} m_3 = 4.6 \times 10^{-2}\,\mathrm{eV} \ \ \text{to} \ \ 5.4 \times 10^{-2}\,\mathrm{eV} .$$

Note that these ranges are rather narrow: m_1 can be only as large as $11/6.4 \sim 1.7$ of its minimum value, and m_3 can be only as large as $54/46 \sim 1.2$ of its minimum value.

After fixing $M_{ee} = 0$, the next step is to specialize either to Class I by imposing $M_{e\mu} = M_{e\tau}$ or to Class II by imposing $M_{\mu\mu} = M_{\tau\tau}$. Either choice will fix the angle θ_1 in terms of the other parameters, thus reducing the number of free parameters to four: the three masses m_i and the angle θ_3.

---

[10]In more detail, the inverted case $m_3 < m_1 < m_2$ would require roughly $|\frac{m_2}{m_1} \tan^2 \theta_3 \pm 1| < 6 \times 10^{-2}$, where the $\pm$ is fixed according to $\tilde{m}_1 \tilde{m}_2 > 0$ (plus sign) or $\tilde{m}_1 \tilde{m}_2 < 0$ (minus sign). For the $+$ case, this inequality is clearly impossible to satisfy since 1 is larger than 10^{-2}. For the minus case, the ratio m_2/m_1 would have to be of order 1 but fine-tuned to two decimal places. We will not consider this particular case and thereby specialize to $m_1 < m_2 < m_3$.

If we were to impose the condition $M_{e\mu} = M_{e\tau}$ (Class I), then this would fix

$$\tan\theta_1 = \frac{1 - xs_2}{1 + xs_2} \quad \text{where} \quad x \equiv \frac{c_3^2 \tilde{m}_1 + s_3^2 \tilde{m}_2 - m_3}{c_3 s_3 (\tilde{m}_2 - \tilde{m}_1)} .$$

Instead, if we were to impose the condition $M_{\mu\mu} = M_{\tau\tau}$ (Class II), then this would fix[11] $\tan\theta_1 = -y + \sqrt{y^2 + 1}$ where

$$y \equiv \frac{(\tilde{m}_1 - \tilde{m}_2)s_2 \sin(2\theta_3)}{c_2^2 m_3 - p\,\tilde{m}_1 - q\,\tilde{m}_2} \quad \text{with} \quad p \equiv s_3^2 - s_2^2 c_3^2 \quad \text{and} \quad q \equiv c_3^2 - s_2^2 s_3^2 .$$

In the limit $\theta_2 \to 0$, the two conditions become equivalent and imply $\theta_1 \to \pi/4$. Therefore the limiting case $\theta_2 \to 0$ of our matrices of Classes I and II corresponds to the $\mu\tau$-symmetric ansatz

$$M_{\mu\tau-\text{sym}} \equiv \begin{pmatrix} 0 & 1 & 1 \\ & a & b \\ & & a \end{pmatrix} \tag{5.2}$$

which along with the possibility of $\theta_1 = \pi/4$ was studied by many authors [17].

At this point we should comment on $\mu\tau$ symmetry in the neutrino mass matrix. Since the mass of the τ is an order of magnitude larger than the mass of the muon, the effective Lagrangian at energy scales below m_τ already exhibits deviations from any underlying $\mu\tau$ symmetry that may exist at high energy. At the energy scale of neutrino masses $m_\nu \ll m_\mu$, any high-energy $\mu\tau$ symmetry should be badly broken, and thus any model that attempts to predict the $\mu\tau$-symmetric texture of (5.2) must show how corrections to M are suppressed at low energy.

It is also worth remarking that tribimaximal mixing implies $M_{e\mu} = M_{e\tau}$ and $M_{\mu\mu} = M_{\tau\tau}$, but the converse is not true. For the $\mu\tau$-symmetric ansatz (5.2), the third eigenvector is $V_{\alpha 3} \propto (0, 1, -1)$, exactly as for tribimaximal mixing, irrespective of the values of a and b. However, the other two eigenvectors are only proportional to $(-2, 1, 1)$ and $(1, 1, 1)$ for the particular case $b = 1 - a$. For example, $a = 5$ and $b = 1 - 5 = -4$ reproduce the matrix $M_{\text{TB}}^{-1,+2,9}$ of Eq. (3.3). On the other hand, changing b to -4.2 gives

$$M = \begin{pmatrix} 0 & 1 & 1 \\ & 5 & -4.2 \\ & & 5 \end{pmatrix} \implies R \approx 36 \quad \text{and} \quad |V_{\text{PMNS}}| \approx \begin{pmatrix} 0.80 & 0.60 & 0 \\ 0.43 & 0.56 & 0.71 \\ 0.43 & 0.56 & 0.71 \end{pmatrix}$$

which deviates from tribimaximal mixing in the first two columns of V. Attempting to increase $|M_{\mu\tau}|$ to 4.3 would result in $R \approx 42$, just above the upper limit, but the resulting V would remain compatible with the bounds in Eq. (1.1).

---

[11]This condition results in a quadratic equation for $\tan\theta_1$ whose two roots are $\tan\theta_1 = -y \pm \sqrt{y^2 + 1}$. We choose the $+$ sign to keep $\tan\theta_1$ positive.

Attempting instead to decrease $|M_{\mu\tau}|$ below 4 results in a mass-squared difference ratio that is too small. For example, $|M_{\mu\tau}| = 3.9$ would result in $R \approx 23$, which is less than the empirical lower bound of 25.5. As for the previous case, the resulting V would be compatible with data.

Thus in the $\mu\tau$-symmetric case, the experimental constraint on $R = m_{31}^2/m_{21}^2$ is more stringent than the constraints for the entries in V. This can be understood from Fig. 1, in which we plot R as a function of $|M_{\mu\tau}|/M_{\mu\mu}$ for the matrix in Eq. (5.2). As $|M_{\mu\tau}|/M_{\mu\mu} \to 1$ we have $m_{21}^2 \to 0$, so that the ratio R diverges as $|M_{\mu\tau}| \to M_{\mu\mu}$, which we will discuss in more detail in the next section (see Eq. (6.1)).

Figure 1: The mass-squared difference ratio $R \equiv m_{31}^2/m_{21}^2$ for the $\mu\tau$-symmetric ansatz Eq. (5.2). The curves correspond to the fixed values $M_{\mu\mu} = 3$ (Thick solid), 4 (Medium solid), 5 (Thin solid), 6 (Dashed), 7 (Dotted). For $|M_{\mu\tau}|/M_{\mu\mu} > 1$, reflect the graph about the vertical line $|M_{\mu\tau}|/M_{\mu\mu} = 1$
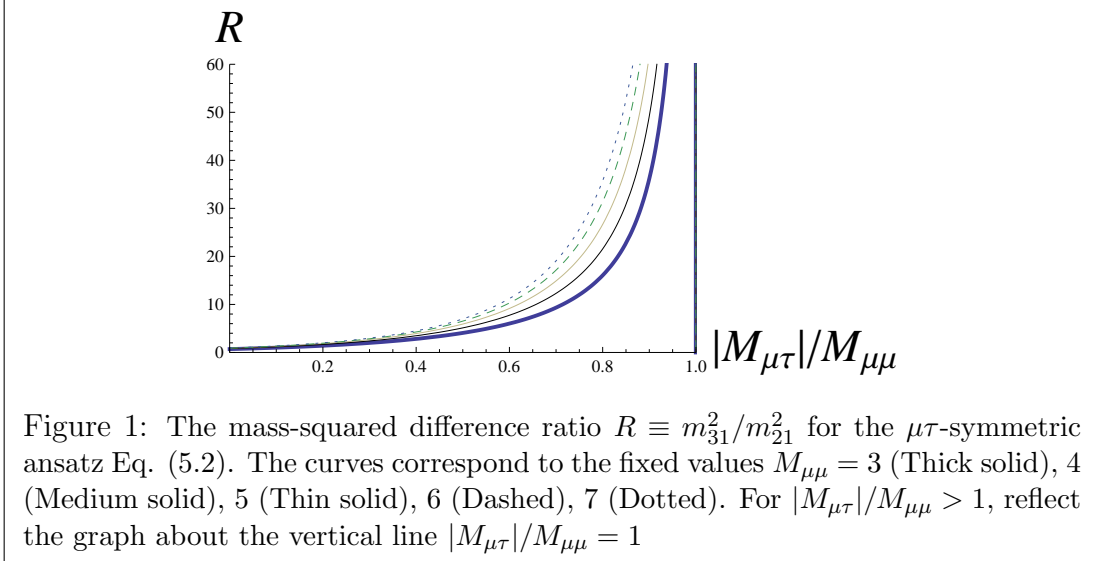
In comparison, there is no divergence in either V_{e1} or V_{e2}, whose sensitivity to the ratio $|M_{\mu\tau}|/M_{\mu\mu}$ is displayed in Figs. 2(a) and 2(b).

Having gained an analytic understanding of the mass matrices in Class I (3.7) and Class II (3.8), as well as their $\mu\tau$-symmetric intersection (5.2), we now turn to numerics.

6 Real Mass Matrices: Class I ($M_{e\mu} = M_{e\tau}$)

We now begin a numerical study of the Class I ansatz defined by Eq. (3.7), which for the convenience of the reader we display again:

$$M_{\mathrm{I}} \equiv \begin{pmatrix} 0 & 1 & 1 \\ & M_{\mu\mu} & M_{\mu\tau} \\ & & M_{\tau\tau} \end{pmatrix}$$

Here $M_{\mu\tau}$ is strictly negative, and all other nonzero entries are strictly positive.

Figure 3(a) shows a plot of the allowed values for the ratio $M_{\mu\mu}/M_{\tau\tau}$ while letting $M_{\mu\tau}$ range over all its possible values. We find that the nonzero diagonal entries can lie in the

Figure 2: The elements V_{e1} and V_{e2} of the mixing matrix for the $\mu\tau$-symmetric ansatz Eq. (5.2). The curves correspond to the fixed values $M_{\mu\mu} = 3$ (Thick solid), 4 (Medi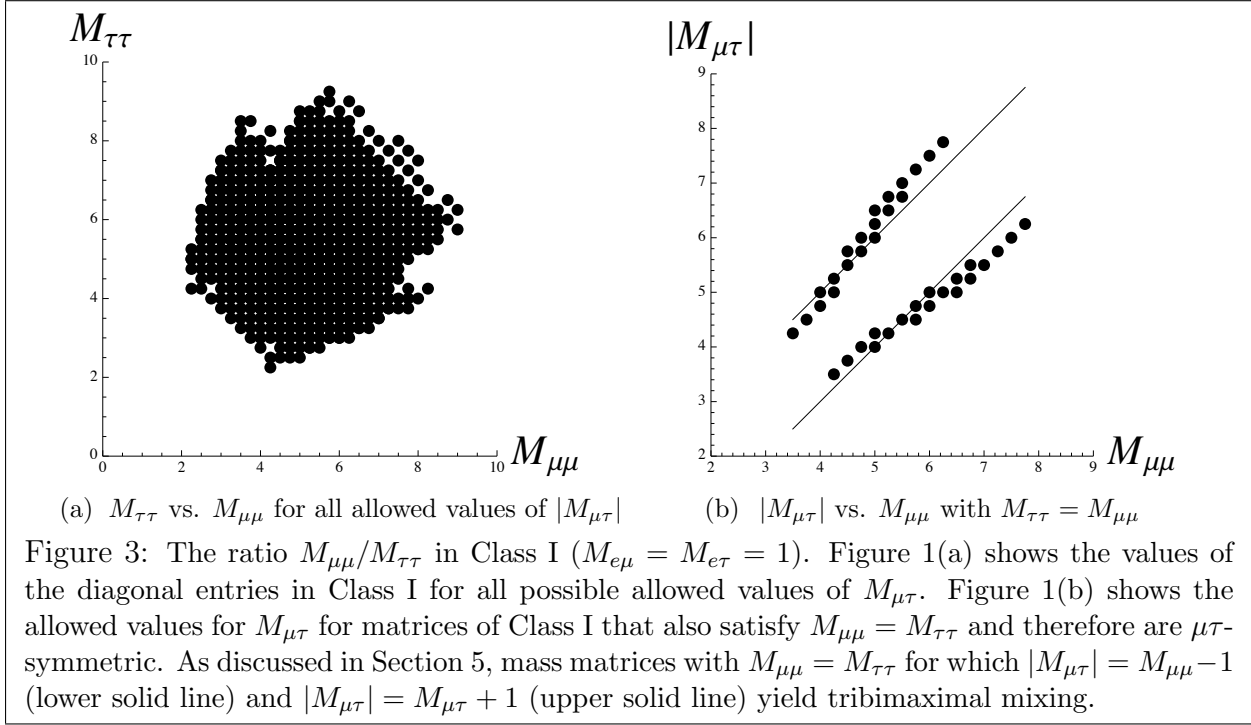um solid), 5 (Thin solid), 6 (Dashed), 7 (Dotted). For $|M_{\mu\tau}|/M_{\mu\mu} > 1$, reflect each graph about the vertical line $|M_{\mu\tau}|/M_{\mu\mu} = 1$.
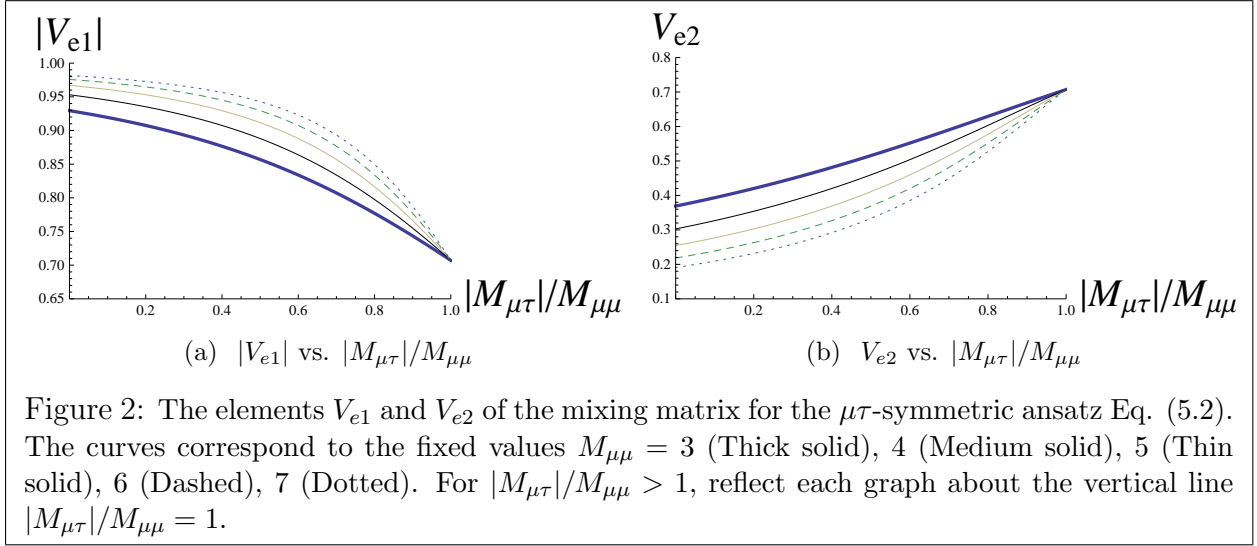
ranges[12] $M_{\mu\mu} \sim 2 - 9$ and $M_{\tau\tau} \sim 2 - 10$. The fact that these ranges are essentially the same is something we already knew, since as discussed in Section 3 the case $M_{\mu\mu} = M_{\tau\tau}$ is the $\mu\tau$-symmetric subcase of Class I.

---

[12]Here and throughout the rest of the paper, we use the "$\sim$" symbol to denote a rough guide for the values of the entries in M, to be compared with either $M_{e\mu} = M_{e\tau} = 1$ (Class I) or $M_{\mu\mu} = M_{\tau\tau} = 5$ (Class II). The idea is to get a feel for what the entries in M can be, and then afterwards to hunt for precise numerical values that fit data.

(a) $M_{\tau\tau}$ vs. $M_{\mu\mu}$ for all allowed values of $|M_{\mu\tau}|$ (b) $|M_{\mu\tau}|$ vs. $M_{\mu\mu}$ with $M_{\tau\tau} = M_{\mu\mu}$

Figure 3: The ratio $M_{\mu\mu}/M_{\tau\tau}$ in Class I ($M_{e\mu} = M_{e\tau} = 1$). Figure 1(a) shows the values of the diagonal entries in Class I for all possible allowed values of $M_{\mu\tau}$. Figure 1(b) shows the allowed values for $M_{\mu\tau}$ for matrices of Class I that also satisfy $M_{\mu\mu} = M_{\tau\tau}$ and therefore are $\mu\tau$-symmetric. As discussed in Section 5, mass matrices with $M_{\mu\mu} = M_{\tau\tau}$ for which $|M_{\mu\tau}| = M_{\mu\mu} - 1$ (lower solid line) and $|M_{\mu\tau}| = M_{\mu\tau} + 1$ (upper solid line) yield tribimaximal mixing.

However, looking at Figure 3(a) in isolation may give the misleading impression that the case $|M_{\mu\tau}| = M_{\mu\mu} = M_{\tau\tau}$ is allowed when in fact it is experimentally ruled out, as can be seen numerically in Figure 3(b). This can also be seen in Figs. 1, 2(a) and 2(b) when compared with the bounds given in Eqs. (1.1) and (1.2).

This can also be understood analytically as follows. The mass matrix

$$M_{\rm B} \equiv \begin{pmatrix} 0 & 1 & 1 \\ & a & -a \\ & & a \end{pmatrix} \tag{6.1}$$

implies a "bimaximal" mixing matrix

$$V_{\rm PMNS} = V_{\rm B} \equiv \begin{pmatrix} \frac{-1}{\sqrt{2}} & \frac{1}{\sqrt{2}} & 0 \\ \frac{1}{2} & \frac{1}{2} & \frac{1}{\sqrt{2}} \\ \frac{1}{2} & \frac{1}{2} & \frac{-1}{\sqrt{2}} \end{pmatrix} \tag{6.2}$$

and two equal neutrino masses, both of which are incompatible with the empirically allowed ranges quoted in (1.1) and (1.2).

Figure 3(b) shows that the set of allowed mass matrices splits into two branches, with larger and smaller $|M_{\mu\tau}|$, which yield a larger and smaller R respectively. For example, for fixed $M_{\mu\mu} = M_{\tau\tau} = 5$ we recover[13] either the matrix with $M_{\mu\tau} = -4$ and $R \approx 27$ in Eq.

---

[13]As discussed in Section 3, we also have Eq. (3.5).

11

(3.3), or the matrix with $M_{\mu\tau} = -6$ and $R = 40$ in Eq. (3.5).

We can use Figures 3(a) and 3(b) to look for examples of mass matrices with non-tribimaximal mixing. Towards the upper limit of $|M_{\mu\tau}| \sim 8$, we find

$$M = \begin{pmatrix} 0 & 1 & 1 \\ & 6 & -7.6 \\ & & 6 \end{pmatrix} \implies R \approx 35 \quad \text{and} \quad |V_{\text{PMNS}}| \approx \begin{pmatrix} 0.86 & 0.50 & 0 \\ 0.36 & 0.61 & 0.71 \\ 0.36 & 0.61 & 0.71 \end{pmatrix} .$$

Like tribimaximal mixing, this case has $M_{e\mu} = M_{e\tau}$ and $M_{\mu\mu} = M_{\tau\tau}$ with $V_{\alpha 3} = (0, \frac{1}{\sqrt{2}}, \frac{-1}{\sqrt{2}})$. Unlike tribimaximal mixing, the second column of V is not proportional to $(1, 1, 1)$, and the first column changes accordingly to maintain orthogonality. This is all consistent with the analytic understanding of the $\mu\tau$-symmetric ansatz from Section 5.

Thus, as emphasized throughout, this is an example with $M_{\mu\mu} = M_{\tau\tau}$ but without tribimaximal mixing. In passing, we mention that increasing $|M_{\mu\tau}|$ to 7.7 would make $|V_{e1}|$ too large and V_{e2} too small with respect to the bounds given in Eq. (1.1). The sensitivity of V_{e1} and V_{e2} to changes in $|M_{\mu\tau}|$ can be seen in Figs. 2(a) and 2(b).

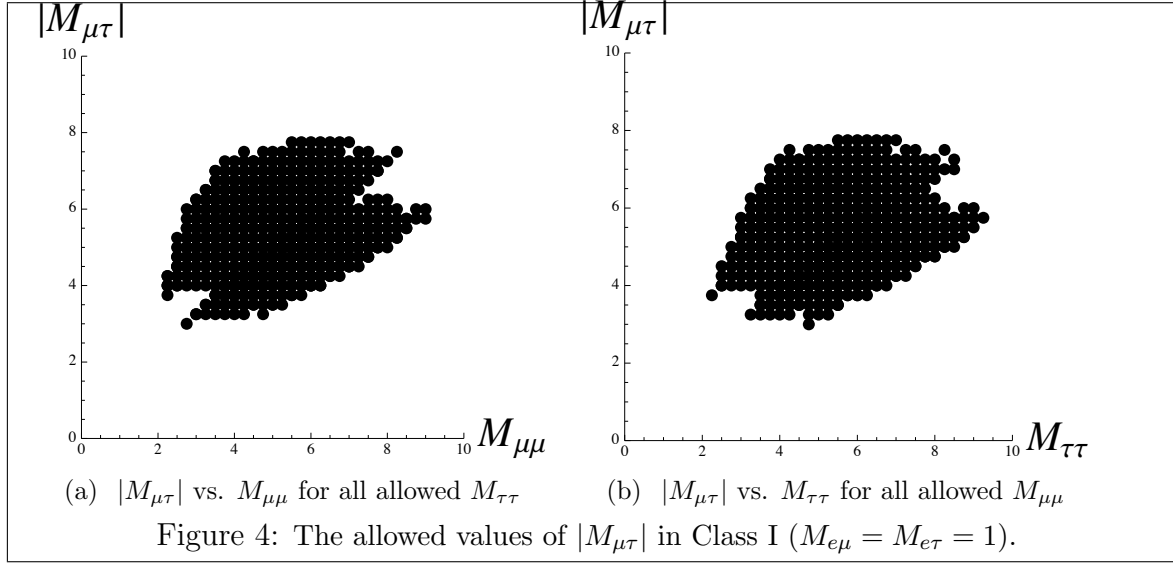Toward the lower limit of $|M_{\mu\tau}| \sim 3$, we find

$$M = \begin{pmatrix} 0 & 1 & 1 \\ & 3 & -2.9 \\ & & 3.9 \end{pmatrix} \implies R \approx 27 \quad \text{and} \quad |V_{\text{PMNS}}| \approx \begin{pmatrix} 0.77 & 0.64 & 0.02 \\ 0.48 & 0.59 & 0.65 \\ 0.42 & 0.49 & 0.76 \end{pmatrix}$$

which is of a similar form to the "nTB" matrix of Eq. (3.6), except with $M_{\tau\tau}$ larger than $M_{\mu\mu} = |M_{\mu\tau}|$. Again in passing, we point out that increasing $|M_{\mu\tau}|$ to 3 would make $|V_{e1}|$ too small and V_{e2} too large. On the other hand, keeping $|M_{\mu\tau}| = 2.9$ but increasing $M_{\tau\tau}$ to 4 would result in $R \approx 25.2$, just below the experimental lower bound, while maintaining a consistent mixing matrix V. An example of the sensitivity of R to the ratios of various entries in M can be seen in Fig. 1, although the matrix above is not $\mu\tau$ symmetric.
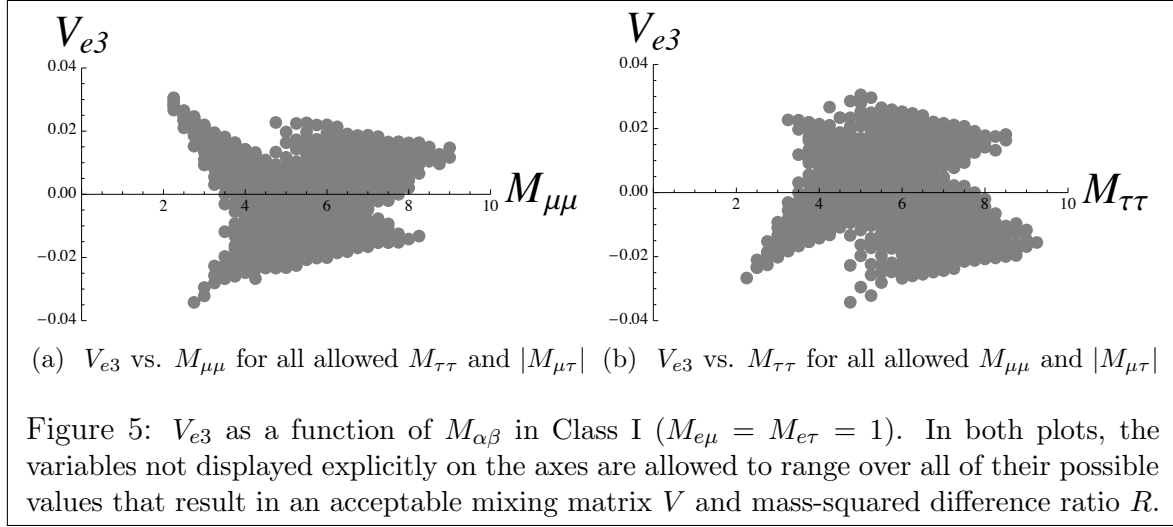
Numerically we find that for all allowed values for $M_{\mu\mu}$ and $M_{\tau\tau}$, the entry $|M_{\mu\tau}|$ can be in the range $\sim 3 - 8$. This can be seen in Figs. 4(a) and 4(b). We conclude the study of Class I with a comment on V_{e3}. Figures 5(a) and 5(b) show that these mass matrices exhibit a maximum value $|V_{e3}| \sim 0.03$, which is rather small. However, these figures also identify that having $M_{\mu\mu}$ and $M_{\tau\tau}$ both less than 3 or greater than 8 ensures a nonzero V_{e3}. Recall that previously we observed $M_{\mu\mu} \sim 2 - 9$ and $M_{\tau\tau} \sim 2 - 10$, so that the narrow ranges $M_{\mu\mu} \sim 2 - 3$ or $8 - 9$, and $M_{\tau\tau} \sim 2 - 3$ or $8 - 10$ are those which necessarily produce $V_{e3} \neq 0$. These ranges are correlated, so that $M_{\mu\mu} \sim 2$ with $M_{\tau\tau} \sim 10$ is not allowed. As an example, we have:

$$M = \begin{pmatrix} 0 & 1 & 1 \\ & 3 & -6.4 \\ & & 7.5 \end{pmatrix} \implies R \approx 29 \quad \text{and} \quad V_{\text{PMNS}} \approx \begin{pmatrix} -0.86 & 0.51 & 0.02 \\ 0.43 & 0.70 & 0.58 \\ 0.28 & 0.50 & -0.82 \end{pmatrix}$$

and thereby generate $|V_{e3}| \sim 0.02$, as for M_{nTB}.

(a) $|M_{\mu\tau}|$ vs. $M_{\mu\mu}$ for all allowed $M_{\tau\tau}$ (b) $|M_{\mu\tau}|$ vs. $M_{\tau\tau}$ for all allowed $M_{\mu\mu}$

Figure 4: The allowed values of $|M_{\mu\tau}|$ in Class I ($M_{e\mu} = M_{e\tau} = 1$).

In summary, matrices of Class I necessarily have "small" values of V_{e3}, reaching a maximum of only ~ 0.03.

(a) V_{e3} vs. $M_{\mu\mu}$ for all allowed $M_{\tau\tau}$ and $|M_{\mu\tau}|$ (b) V_{e3} vs. $M_{\tau\tau}$ for all allowed $M_{\mu\mu}$ and $|M_{\mu\tau}|$

Figure 5: V_{e3} as a function of $M_{\alpha\beta}$ in Class I ($M_{e\mu} = M_{e\tau} = 1$). In both plots, the variables not displayed explicitly on the axes are allowed to range over all of their possible values that result in an acceptable mixing matrix V and mass-squared difference ratio R.
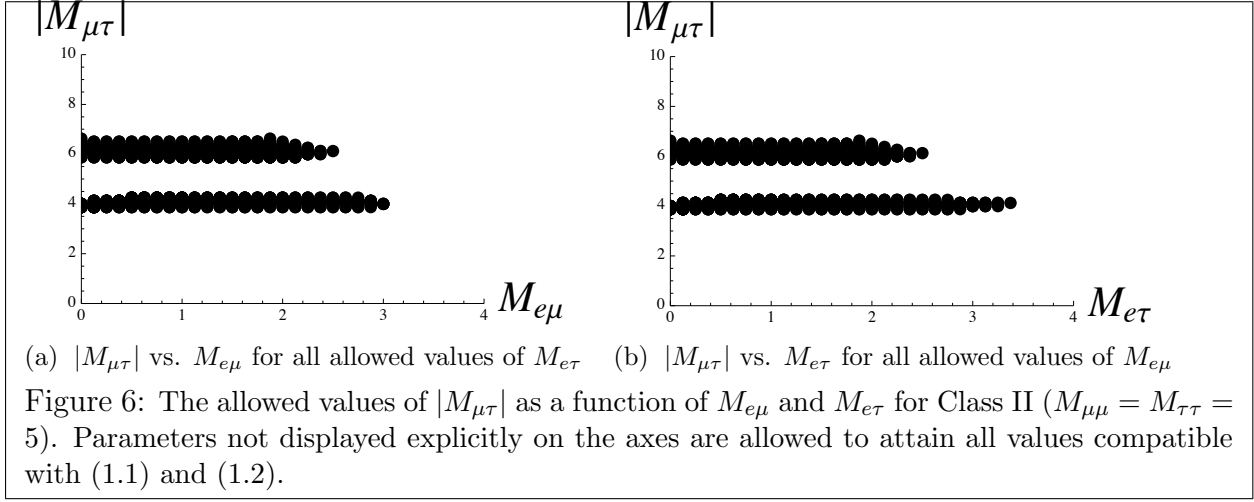
7   Real Mass Matrices: Class II ($M_{\mu\mu} = M_{\tau\tau}$)

Now consider matrices from Class II, which is defined by

$$M_{\mathrm{II}} \equiv \begin{pmatrix} 0 & M_{e\mu} & M_{e\tau} \\ & 5 & M_{\mu\tau} \\ & & 5 \end{pmatrix} .$$

In Figures 6(a) and 6(b) we plot the allowed values of $|M_{\mu\tau}|$ as a function of $M_{e\mu}$ and $M_{e\tau}$. We find that $|M_{\mu\tau}|$ is constrained to be very close to either 4 or 6, reminiscent of the

13

tribimaximal cases given in Eqs. (3.3) and (3.5). This tells us that matrices in Class II necessarily exhibit near tribimaximal mixing if the ratio $M_{e\mu}/M_{e\tau}$ is close to 1, and if both $M_{e\mu}$ and $M_{e\tau}$ are close[14] to 1.

(a) $|M_{\mu\tau}|$ vs. $M_{e\mu}$ for all allowed values of $M_{e\tau}$ (b) $|M_{\mu\tau}|$ vs. $M_{e\tau}$ for all allowed values of $M_{e\mu}$

Figure 6: The allowed values of $|M_{\mu\tau}|$ as a function of $M_{e\mu}$ and $M_{e\tau}$ for Class II ($M_{\mu\mu} = M_{\tau\tau} = 5$). Parameters not displayed explicitly on the axes are allowed to attain all values compatible with (1.1) and (1.2).

We emphasize that the reason the ratio $M_{e\mu}/M_{e\tau}$ characterizes proximity to tribimaximal mixing in Class II is simply because the data in (1.1) and (1.2) constrain $|M_{\mu\tau}|$ to be close to 4 or 6 (in units for which $M_{\mu\mu} = M_{\tau\tau} = 5$). Otherwise, as discussed below Eq. (5.2), $\mu\tau$ symmetry does not imply tribimaximal mixing.

In Figure 7 we examine the ratio $M_{e\mu}/M_{e\tau}$. The case $M_{e\mu}/M_{e\tau} = 1$ is allowed for $M_{e\mu} = M_{e\tau} \sim 0.8 - 1.5$, but for values out of this range for either $M_{e\mu}$ or $M_{e\tau}$, the mixing matrix will deviate significantly from the tribimaximal ansatz while still fitting data.
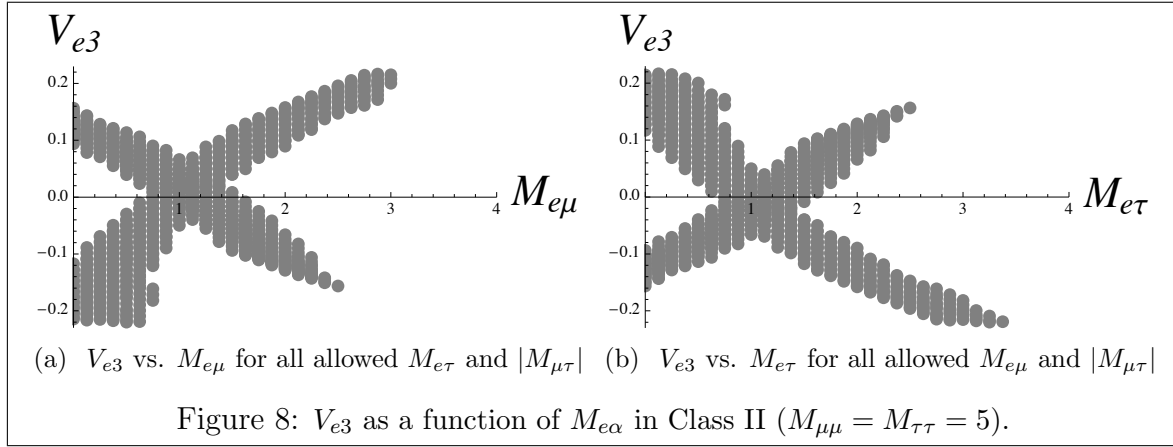

Figure 7: The ratio $M_{e\tau}/M_{e\mu}$ (for all allowed $|M_{\mu\tau}|$) in Class II ($M_{\mu\mu} = M_{\tau\tau} = 5$).

---
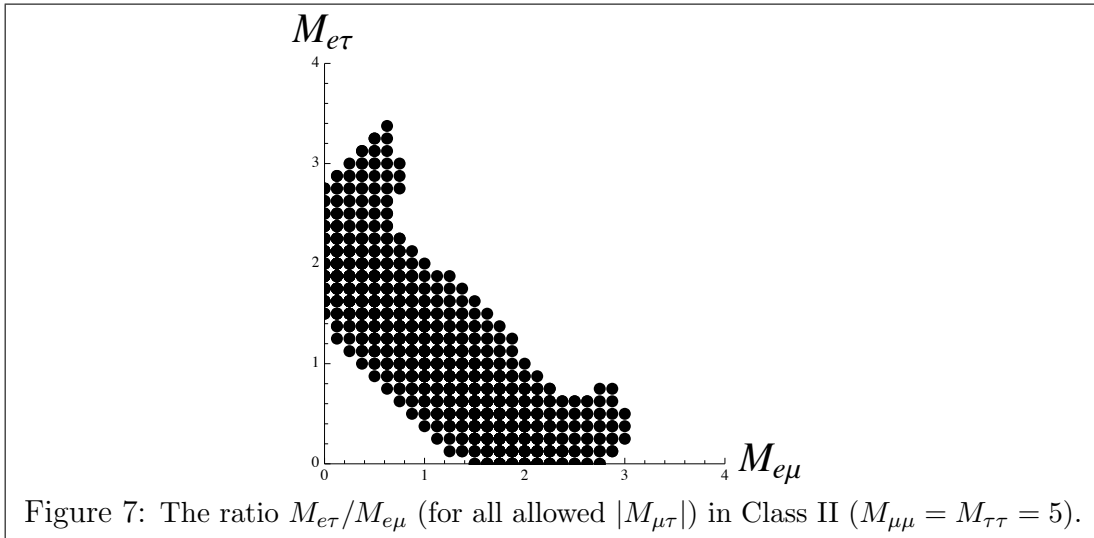
[14]In other words, $M_{e\mu}/M_{\mu\mu} \sim M_{e\tau}/M_{\mu\mu} \sim \frac{1}{5}$.

In particular, it is possible for matrices of Class II ($M_{\mu\mu} = M_{\tau\tau}$, $M_{e\mu} \neq M_{e\tau}$) to fit data with either $M_{e\mu} = 0$ or $M_{e\tau} = 0$ but not both. For example:

$$M = \begin{pmatrix} 0 & 0 & 1.4 \\ & 5 & -4 \\ & & 5 \end{pmatrix} \implies R \approx 41 \quad \text{and} \quad |V_{\text{PMNS}}| \approx \begin{pmatrix} 0.86 & 0.50 & 0.11 \\ 0.29 & 0.66 & 0.69 \\ 0.42 & 0.56 & 0.71 \end{pmatrix}.$$

Decreasing $M_{e\tau}$ to 1.3 would make R and $|V_{e1}|$ too large and V_{e2} too small with respect to the bounds in Eq. (1.1). This two-zero texture is labeled "Case A_1" in a study by Frampton, Glashow and Marfatia about possible zeros in the neutrino mass matrix in the flavor basis [18]. The salient feature of both their work and ours is the possibility of a "large" V_{e3}, on which we now elaborate.

(a) V_{e3} vs. $M_{e\mu}$ for all allowed $M_{e\tau}$ and $|M_{\mu\tau}|$ (b) V_{e3} vs. $M_{e\tau}$ for all allowed $M_{e\mu}$ and $|M_{\mu\tau}|$

Figure 8: V_{e3} as a function of $M_{e\alpha}$ in Class II ($M_{\mu\mu} = M_{\tau\tau} = 5$).

For either $M_{e\mu}$ or $M_{e\tau}$ less than ~ 0.6 or greater than ~ 1.6 in Class II, a nonzero V_{e3} is generated. Figures 8(a) and 8(b) show that the empirical upper limit $|V_{e3}| \sim 0.2$ can be generated for $M_{e\mu}$ or $M_{e\tau}$ close to ~ 0 or 3. Using these along with Figure 7, we find:

$$M = \begin{pmatrix} 0 & 0.2 & 3 \\ & 5 & -4 \\ & & 5 \end{pmatrix} \implies R \approx 33 \quad \text{and} \quad |V_{\text{PMNS}}| \approx \begin{pmatrix} 0.79 & 0.57 & 0.22 \\ 0.32 & 0.69 & 0.65 \\ 0.52 & 0.44 & 0.73 \end{pmatrix}.$$

Decreasing $M_{e\mu}$ to zero would generate $|V_{e3}| \approx 0.23$, which is too large if we believe the upper bound given in Eq. (1.1).

In summary, mass matrices of Class II can result in values for $|V_{e3}|$ anywhere from 0 to the empirical upper limit of ~ 0.22. In particular, when the ratio $M_{e\mu}/M_{e\tau}$ is greater than ~ 2 or less than $\sim 1/2$, a "large" $|V_{e3}|$ is necessarily generated.

8   CP Violation

We will now allow for the possibility that the neutrino mass matrix violates CP. As discussed in Section 4, any 3-by-3 complex symmetric mass matrix with $M_{ee} = 0$ can be rephased into

15

the form of Eq. (4.2), which we repeat for convenience:

$$M = \begin{pmatrix} 0 & |M_{e\mu}| & |M_{e\tau}|\,e^{i\varphi} \\ & |M_{\mu\mu}| & |M_{\mu\tau}|\,e^{i\eta} \\ & & |M_{\tau\tau}| \end{pmatrix} \,.$$

We need to diagonalize M to determine how φ and η contribute to the CP-violating angle $\delta_{\rm CP}$ and to the Majorana phase angles ρ and σ. (Recall the notation of Eq. (1.3).) The mapping of two phases φ and η to three observables $\delta_{\rm CP}$, ρ and σ is explained by the fact that ρ and σ are not independent parameters when $M_{ee} = 0$. With a complex mass matrix, the condition $M_{ee} = 0$ implies

$$\tan^2\theta_2 = -\left(\frac{c_3^2\,e^{-i2\rho}m_1 + s_3^2 e^{-i2\sigma}m_2}{m_3}\right) \tag{8.1}$$

which is the generalization of Eq. (5.1) with the possibility of ρ and σ being different from 0 or $\pi/2$. The imaginary part of this fixes ρ in terms of σ through the relation

$$\frac{\sin(2\rho)}{\sin(2\sigma)} = -\tan^2\theta_3\,\frac{m_2}{m_1} \tag{8.2}$$

so that only one of these phases is an independent parameter.

The main result of the generalization to complex mass matrices is that nontrivial phases open up new regions for the allowed values of $|M_{\alpha\beta}|$.

To understand this claim it is sufficient to specialize to the following example: Recall the matrix $M_{\rm B}$ from Eq. (6.1), which predicted $m_1 = m_2$ and bimaximal mixing with $|V_{e1}| = V_{e2}$, which are incompatible with the bounds in (1.1) and (1.2). Generalizing this matrix to the complex case

$$M_{\rm Bc} \equiv \begin{pmatrix} 0 & 1 & e^{i\varphi} \\ & a & a\,e^{i\eta} \\ & & a \end{pmatrix} \tag{8.3}$$

can split the degeneracy $m_1 = m_2$ and modify $|V_{e1}| = V_{e2}$ significantly enough to become compatible with oscillation data. In the next section, we will show that the matrix $M_{\rm Bc}$ can result in tribimaximal mixing with $m_i = (1, 2, 9)$ and $m_i = (1, 2, 11)$, just as in the CP-conserving case discussed in Section 3.

9   Tribimaximal Mixing and Nonzero Majorana Phases

Consider tribimaximal mixing[15], meaning $V_{\rm PMNS} = V_{\rm TB}$, but with arbitrary Majorana phases so that[16] $M = V^*DV^\dagger$ is complex even though $\delta_{\rm CP}$ drops out since $V_{e3} = 0$.

---

[15]Some of our work in this section overlaps with that of Z. Z. Xing [9].

[16]We remind the reader that $D = {\rm diag}(m_1, m_2, m_3)$ is real and positive, and $V = \mathcal{K}V_{\rm PMNS}\mathcal{M}$ is the full 3-by-3 unitary matrix including the extra phases in $\mathcal{K}$ and $\mathcal{M}$. If $\vec{v}_i$ denotes the $i^{\rm th}$ column of V, then $M = V^*DV^\dagger = \sum_{i=1} m_i \vec{v}_i^* \vec{v}_i^\dagger$.

For tribimaximal mixing with arbitrary Majorana phases, the condition $M_{ee} = 0$ now fixes

$$2m_1 e^{-i2\rho} + m_2 e^{-i2\sigma} = 0 \tag{9.1}$$

which corresponds to taking $\theta_2 = 0$ and $\theta_3 = \sin^{-1}(1/\sqrt{3})$ in Eq. (8.1). This implies

$$m_2 = 2m_1 \quad \text{and} \quad \rho = \sigma + (2n - 1)\frac{\pi}{2} \tag{9.2}$$

where n is any integer. Consider the case $\rho = -\sigma = -\pi/4$. Upon choosing the κ_i as given above Eq. (4.2), we find a rephased mass matrix $\hat{M}$ of the form[17]

$$\hat{M} = M_{\mathrm{TBc}} \equiv \begin{pmatrix} 0 & 1 & 1 \\ & a & a\,e^{i\eta} \\ & & a \end{pmatrix} \tag{9.3}$$

where

$$a = \frac{1}{2}\sqrt{m_3^2 + 1} \quad \text{and} \quad \eta = \pi + \tan^{-1}\left(\frac{2m_3}{m_3^2 - 1}\right). \tag{9.4}$$

As displayed above, this matrix has[18] $\varphi = 0$. We have set the overall scale $m_\nu = m_1 = \hat{M}_{e\mu} = \hat{M}_{e\tau}$ to 1.

For $(m_1, m_2) = (1, 2)$ we can invert the definition $R \equiv m_{31}^2/m_{21}^2$ to get $m_3 = \sqrt{3R + 1}$ and thus obtain the parameters a and η as a function purely of the experimentally constrained ratio R:

$$a = \frac{1}{2}\sqrt{3R + 2} \quad \text{and} \quad \eta = \tan^{-1}\left(\frac{2}{3R}\sqrt{3R + 1}\right) \tag{9.5}$$

where $25.5 \leq R \leq 41.0$ as given in Eq. (1.2). These parameters are plotted as a function of R in Figs. 9(a) and 9(b). In units of $m_1 = 1$, the mass of the heaviest neutrino is $8.80 \leq m_3 \leq 11.1$.

Consider the two examples $m_3 = 9$ and $m_3 = 11$. For $m_i = (1, 2, 9)$ we have $a \approx 4.5$ and $\eta - \pi \approx 0.22$, and for $m_i = (1, 2, 11)$ we have $a \approx 5.5$ and $\eta - \pi \approx 0.18$. This interpolates between the two branches $|M_{\mu\tau}| \sim 4$ and $|M_{\mu\tau}| \sim 6$ of the real-valued tribimaximal mass matrix. For instance, $m_i = (1, 2, 10)$ (so that $R = 33$ exactly) implies $a = \frac{1}{2}\sqrt{101} \approx 5.0$ and $\eta - \pi \approx 0.20$.

Therefore in addition to the CP-conserving case with $\varphi = 0$, $\eta = \pi$ and $|M_{\mu\tau}| \neq M_{\mu\mu}$, we find a new class of allowed tribimaximal mass matrices with $\varphi = 0$, $\eta \sim \pi + 0.2$ and $|M_{\mu\tau}| = M_{\mu\mu}$. It is important to note that, in contrast, the case $\eta \sim 0.2$ is not allowed unless the angle φ is changed to $\sim \pi$. (Recall the notation of Eq. (8.3).) This should be understood in the context of the discussion below Eq. (4.3), in which we showed that phases of $e^{\pm i\pi} = -1$ can be exchanged between $M_{e\tau}$ and $M_{\mu\tau}$.

---

[17]Since M_{TBc} is a complex symmetric matrix, one must take the eigenvalues and eigenvectors of the hermitian matrix $H_{\mathrm{TBc}} \equiv (M_{\mathrm{TBc}})^\dagger M_{\mathrm{TBc}}$ when computing the neutrino masses and mixing angles.

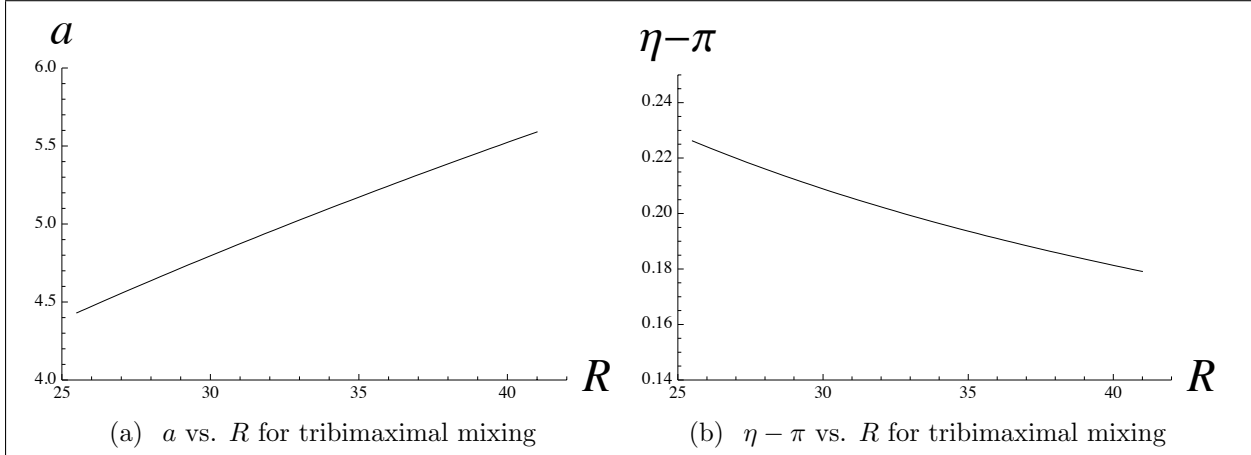[18]As discussed below Eq. (4.3), we can equivalently set $\varphi = \pi$ if we subtract π from η.

(a) a vs. R for tribimaximal mixing

(b) $\eta - \pi$ vs. R for tribimaximal mixing

Figure 9: The parameters $a \equiv M_{\mu\mu} = M_{\tau\tau} = |M_{\mu\tau}|$ and $\eta \equiv \arg(M_{\mu\tau})$ in the matrix M_{Bc} given in Eq. (8.3), for the particular case in which the mixing matrix is exactly tribimaximal. In this case we have $m_2 = 2m_1$ and $M_{e\mu} = M_{e\tau} = m_1$, so that setting $M_{e\mu} = M_{e\tau} = 1$ implies $m_1 = 1$, $m_2 = 2$ and thus $8.80 \le m_3 = \sqrt{3R + 1} \le 11.1$.

10   Complex Mass Matrices with $M_{e\mu} = |M_{e\tau}|$ and $M_{\mu\mu} = M_{\tau\tau} = |M_{\mu\tau}|$

We now turn to a numerical study of the matrix M_{Bc} given in Eq. (8.3). Up to the phases, this is the $\mu\tau$-symmetric subcase of both Classes I and II with the additional condition $|M_{\mu\tau}| = M_{\mu\mu}$. (Note that for non-tribimaximal mixing, the phase φ is no longer necessarily zero or π.) An immediate striking feature of this matrix is given in Figure 10(b), which shows that $|\eta|$ can take essentially only two possible values: ~ 0.2 and $\sim \pi$. This corroborates the intuition we gained from tribimaximal mixing with $|M_{\mu\tau}| = M_{\mu\mu}$.
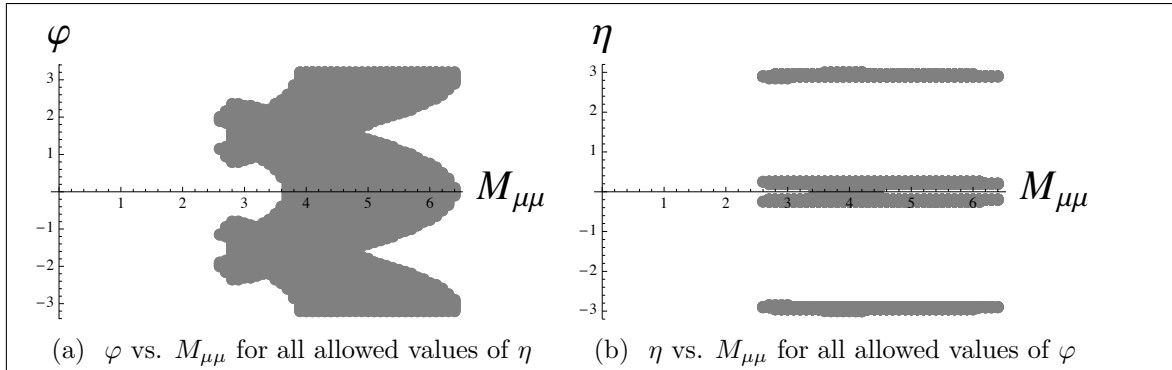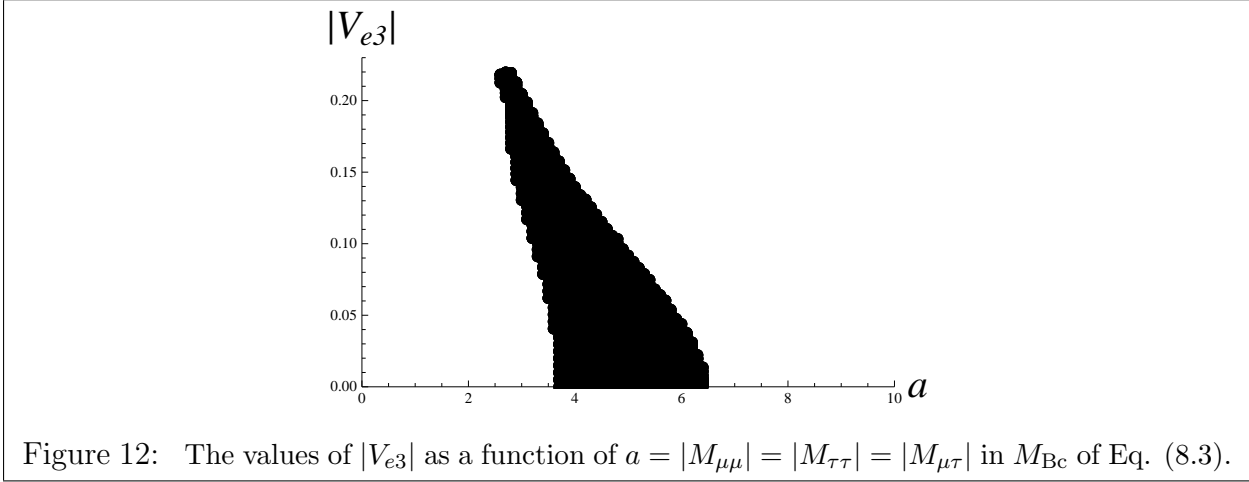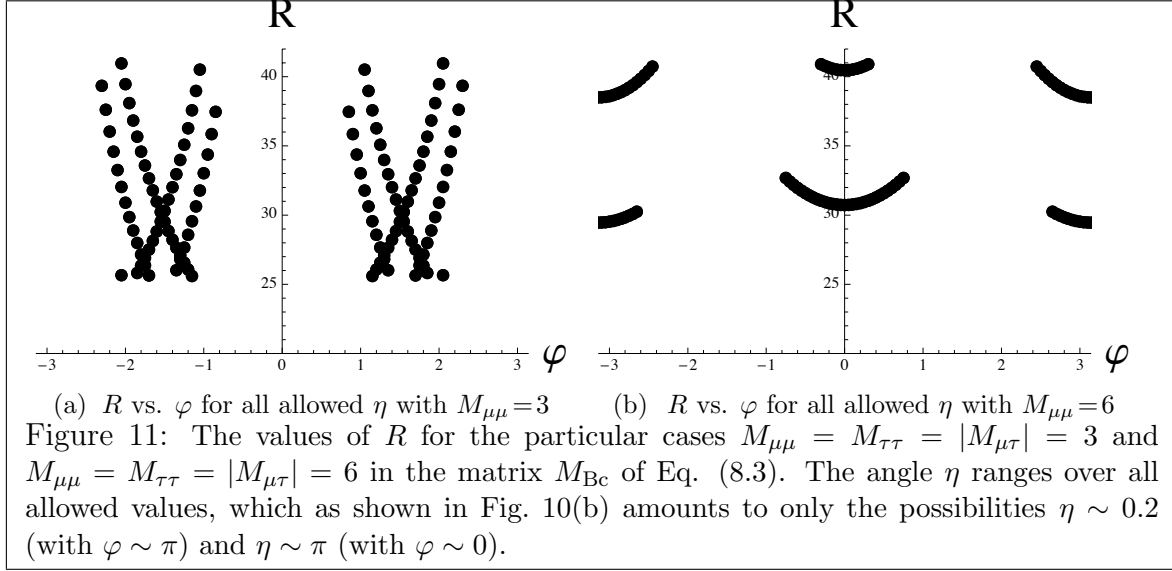

(a) φ vs. $M_{\mu\mu}$ for all allowed values of η

(b) η vs. $M_{\mu\mu}$ for all allowed values of φ

Figure 10: The phase angles as a function of $M_{\mu\mu} = M_{\tau\tau} = |M_{\mu\tau}|$ for the matrix M_{Bc} given in Eq. (8.3). The values near $\eta = \pm 0.2$ in (b) should be understood in the context of the discussion below Eq. (4.3). That is, the allowed values $(\varphi, \eta) = (0, \pm(\pi + 0.2))$ are phenomenologically equivalent to the values $(\varphi, \eta) = (\pi, \pm 0.2)$. In contrast, the values $(\varphi, \eta) = (0, \pm 0.2)$ are not compatible with the data in Eqs. (1.1) and (1.2).
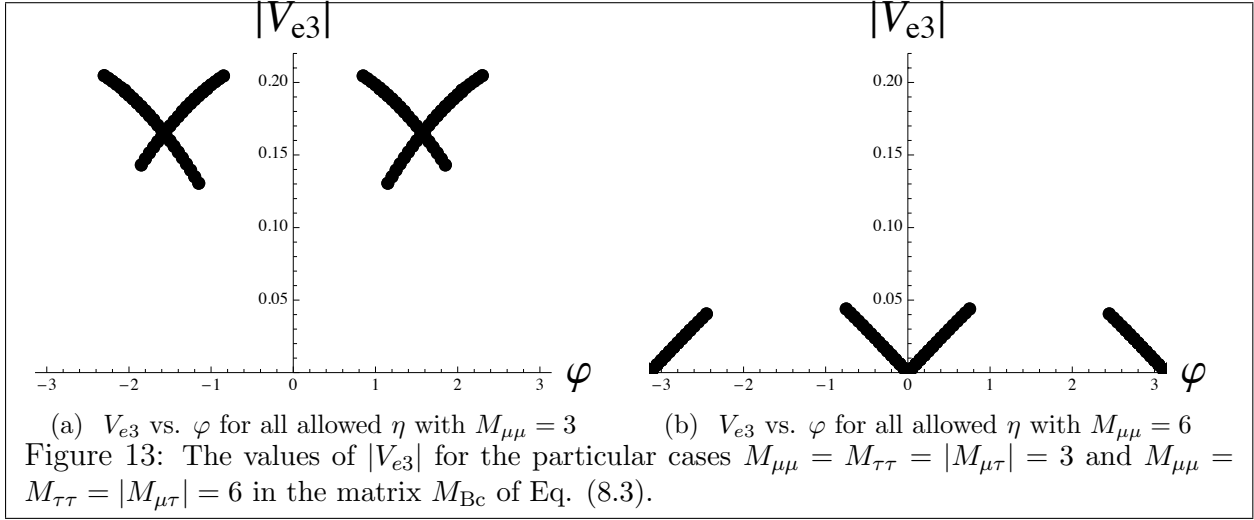
Figures 11(a) and 11(b) show that this CP-violating matrix interpolates between the

18

real-valued cases with $|M_{\mu\tau}| = 4$ and $|M_{\mu\tau}| = 6$, which give $R \approx 27$ and $R = 40$ respectively.

(a) R vs. φ for all allowed η with $M_{\mu\mu} = 3$ (b) R vs. φ for all allowed η with $M_{\mu\mu} = 6$

Figure 11: The values of R for the particular cases $M_{\mu\mu} = M_{\tau\tau} = |M_{\mu\tau}| = 3$ and $M_{\mu\mu} = M_{\tau\tau} = |M_{\mu\tau}| = 6$ in the matrix M_{Bc} of Eq. (8.3). The angle η ranges over all allowed values, which as shown in Fig. 10(b) amounts to only the possibilities $\eta \sim 0.2$ (with $\varphi \sim \pi$) and $\eta \sim \pi$ (with $\varphi \sim 0$).

Figure 12: The values of $|V_{e3}|$ as a function of $a = |M_{\mu\mu}| = |M_{\tau\tau}| = |M_{\mu\tau}|$ in M_{Bc} of Eq. (8.3).

Recall that the matrix M_{Bc} of Eq. (8.3) for the special case $\varphi = 0$ and $\eta = \pi$ reduces to the matrix M_{B} of Eq. (6.1), which implies a bimaximal mixing matrix and thus $|V_{e1}| = V_{e2}$, which is incompatible with the bounds given in (1.1). We find that complex phases can generate mixing matrices that fall in the empirically allowed range $0.14 \leq |V_{e1}| - V_{e2} \leq 0.36$.

The angular parameterization of the mixing matrix makes clear that δ_{CP} only contributes to neutrino oscillations when $V_{e3} \neq 0$. Figures 12, 13(a) and 13(b) show that the magnitude of V_{e3} depends strongly on the value of $a \equiv |M_{\mu\tau}| = M_{\mu\mu} = M_{\tau\tau}$ in mass matrices with $M_{ee} = 0$ and $M_{e\mu} = |M_{e\tau}| \equiv 1$.

19

(a) V_{e3} vs. φ for all allowed η with $M_{\mu\mu} = 3$ (b) V_{e3} vs. φ for all allowed η with $M_{\mu\mu} = 6$

Figure 13: The values of $|V_{e3}|$ for the particular cases $M_{\mu\mu} = M_{\tau\tau} = |M_{\mu\tau}| = 3$ and $M_{\mu\mu} = M_{\tau\tau} = |M_{\mu\tau}| = 6$ in the matrix M_{Bc} of Eq. (8.3).

More generally, amplitudes for CP-violating oscillation processes are proportional to the rephasing-invariant quantity $J \equiv -\mathrm{Im}(V_{e3}V_{\mu2}V_{e2}^*V_{\mu3}^*)$ [19]. Figures 14(a) and 14(b) show that, like V_{e3}, the quantity J also depends strongly on the value of a. For a near its lower bound of ~ 3, the quantity J is of order $\sim 10^{-2}$, but for larger $a \sim 6$ we find that J is at most $\sim 10^{-5}$ and can drop to zero. For an example with a large $|V_{e3}|$ and nonzero δ_{CP}, and hence a large J, we find:
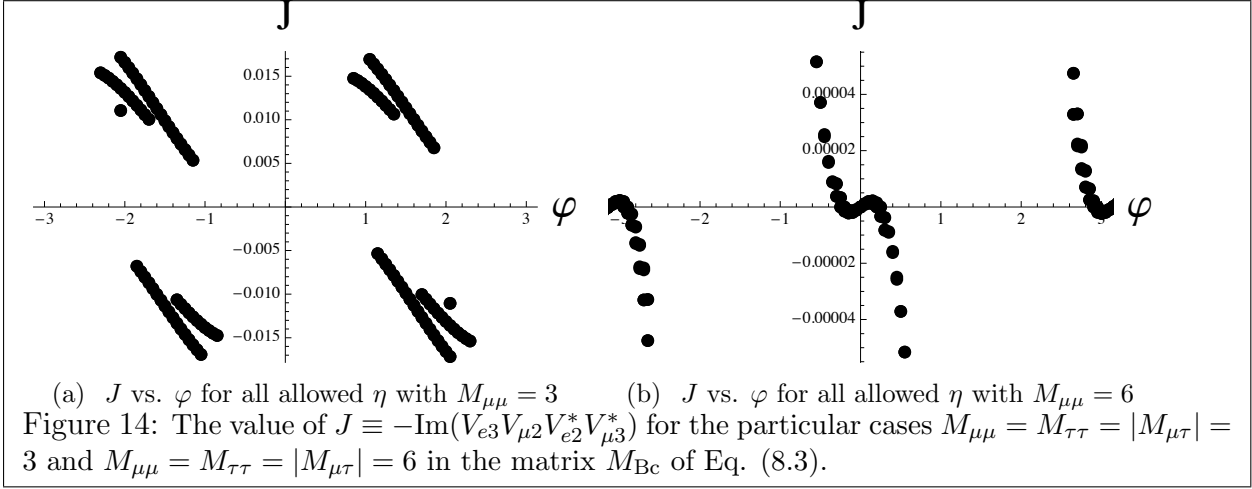
$$
M = \begin{pmatrix} 0 & 1 & e^{i1.1} \\ & 3 & 3\,e^{i0.2} \\ & & 3 \end{pmatrix} \implies R \approx 39 \quad \text{and} \quad |V_{\mathrm{PMNS}}| = \begin{pmatrix} 0.79 & 0.58 & 0.19 \\ 0.52 & 0.50 & 0.70 \\ 0.32 & 0.65 & 0.69 \end{pmatrix}
$$

with $\delta_{\mathrm{CP}} \approx -0.38$ and $J \approx 1.6 \times 10^{-2}$. In contrast, by increasing $|M_{\mu\tau}| = M_{\mu\mu} = M_{\tau\tau}$ to 6 we find

$$
M = \begin{pmatrix} 0 & 1 & e^{i2.8} \\ & 6 & 6\,e^{i0.2} \\ & & 6 \end{pmatrix} \implies R \approx 39 \quad \text{and} \quad |V_{\mathrm{PMNS}}| = \begin{pmatrix} 0.83 & 0.55 & 0.02 \\ 0.40 & 0.58 & 0.71 \\ 0.38 & 0.60 & 0.71 \end{pmatrix}
$$

with $\delta_{\mathrm{CP}} \approx -2.7 \times 10^{-3}$ and $J \approx 1.3 \times 10^{-5}$. These two examples were chosen intentionally to yield the same value for R. Note that for $|M_{\mu\tau}| = M_{\mu\mu} = M_{\tau\tau} = 6$, keeping $\varphi = 1.1$ would result in $R \approx 64$ with $|V_{e1}| \approx 0.90$, both of which are too large, and in $V_{e2} \approx 0.43$, which is too small. On the other hand, the other entries in V_{PMNS} would all stay within the empirically allowed ranges.

In summary, we learn that for the matrix M_{Bc} decreasing the value of $M_{\mu\mu}/M_{e\mu}$ increases the value of $|V_{e3}|$ and thereby results in the possibility for larger amplitudes for CP-violating processes.

20

(a) J vs. φ for all allowed η with $M_{\mu\mu} = 3$ (b) J vs. φ for all allowed η with $M_{\mu\mu} = 6$

Figure 14: The value of $J \equiv -\text{Im}(V_{e3}V_{\mu2}V_{e2}^*V_{\mu3}^*)$ for the particular cases $M_{\mu\mu} = M_{\tau\tau} = |M_{\mu\tau}| = 3$ and $M_{\mu\mu} = M_{\tau\tau} = |M_{\mu\tau}| = 6$ in the matrix M_{Bc} of Eq. (8.3).

11 Discussion

We have studied three types of neutrino mass matrices in the flavor basis with $M_{ee} = 0$. The first two types are the CP-conserving matrices of Class I ($M_{e\mu} = M_{e\tau}$) and of Class II ($M_{\mu\mu} = M_{\mu\tau}$), which we display again for the convenience of the reader (see (3.7) and (3.8)):

$$M_{\text{I}} \equiv \begin{pmatrix} 0 & 1 & 1 \\ & M_{\mu\mu} & M_{\mu\tau} \\ & & M_{\tau\tau} \end{pmatrix} \quad \text{and} \quad M_{\text{II}} \equiv \begin{pmatrix} 0 & M_{e\mu} & M_{e\tau} \\ & 5 & M_{\mu\tau} \\ & & 5 \end{pmatrix} \tag{11.1}$$

The intersection of these two classes is the $\mu\tau$-symmetric ansatz (see (5.2))

$$M_{\mu\tau\text{-sym}} \equiv \begin{pmatrix} 0 & 1 & 1 \\ & a & b \\ & & a \end{pmatrix} . \tag{11.2}$$

The salient phenomenological distinction between Classes I and II is that mass matrices of Class I can accommodate only a small V_{e3} up to ~ 0.03 (Figs. 5(a) and 5(b)), while mass matrices of Class II can predict an arbitrarily large V_{e3} (Figs. 8(a) and 8(b)). Thus fundamental theories which predict a neutrino mass matrix with $M_{\mu\mu} \sim M_{\tau\tau}$ and either $M_{e\mu} \ll M_{e\tau}$ or $M_{e\mu} \gg M_{e\tau}$ (as opposed to $M_{e\mu} \sim M_{e\tau}$) will be the most constrained by future measurements of V_{e3}.

The third type of matrix we studied is the complex matrix (see (8.3))

$$M_{\text{Bc}} \equiv \begin{pmatrix} 0 & 1 & e^{i\varphi} \\ & a & a\,e^{i\eta} \\ & & a \end{pmatrix} . \tag{11.3}$$

For this matrix, smaller values of a result in larger values of V_{e3} and $J \equiv -\text{Im}(V_{e3}V_{\mu2}V_{e2}^*V_{\mu3}^*)$, and thus provide experimentally promising signals of CP violation in neutrino oscillations

21

(Figs. 13(a) and 14(a)). In contrast, larger values of a drive V_{e3} and J to zero (Figs. 13(b) and 14(b)).

A particularly interesting example is obtained from M_{Bc} for the particular case $\varphi = 0$ with

$$a = \frac{1}{2}\sqrt{m_3^2 + 1} \quad \text{and} \quad \eta = \pi + \tan^{-1}\left(\frac{2m_3}{m_3^2 - 1}\right) . \tag{11.4}$$

Here m_3 is the mass of the heaviest neutrino in units of the lighest neutrino ($m_3 > m_2 > m_1$), and the other two masses are $(m_1, m_2) = (1, 2)$. In this case the mixing matrix is exactly tribimaximal, even though $M_{\mu\mu} = M_{\tau\tau} = |M_{\mu\tau}|$. (See Section 9.)

References

[1] R. N. Mohapatra et al, "Theory of Neutrinos: A White Paper," Rept.Prog.Phys.70:1757-1867,2007 (arXiv:hep-ph/0510213v2)

[2] M. C. Gonzalez-Garcia and M. Maltoni, "Phenomenology with Massive Neutrinos," Phys.Rept.460:1-129,2008 (arXiv:0704.1800v2 [hep-ph])

[3] M. C. Gonzalez-Garcia, M. Maltoni and J. Salvado, "Updated global fit to three neutrino mixing: status of the hints of theta13 > 0," JHEP 04 (2010) 056 (arXiv:1001.4524v3 [hep-ph])

[4] L.-L. Chau and W.-Y. Keung, "Comments on the Parametrization of the Kobayashi-Maskawa Matrix," Phys. Rev. Lett. 53, 1802 (1984) ; C. Jarlskog, "A Recursive Parameterisation of Unitary Matrices," arxiv:math-ph/0504049v3 21 Apr 2005.

[5] S. M. Bilenky, "Neutrinoless Double Beta Decay," A report at the Workshop in Particle Physics "Rencontres de Physique de La Vallee d'Aoste", La Thuile, Aosta Valley, February 29-March 6, 2004 (arXiv:hep-ph/0403245v1).

[6] Y. B. Zel'dovich and M. Y. Khlopov, "Study of the neutrino mass in a double β decay," Pis'ma v ZhETF (1981), V.54, PP. 128-151. [English translation: JETP Lett. (1981) V.34, no.3, PP. 141-145]; Y. B. Zel'dovich and M. Y. Klhopov, "The neutrino mass in elementary-particle physics and in big bang cosmology," Usp. Fiz. Nauk (1981) V. 135, PP. 45-74. [English translation: Sov. Phys. Uspekhi (1981) V.24, PP.755-774].

[7] T. Fukuyama and H. Nishiura, "Mass Matrix of Majorana Neutrinos," Ritsumei-pp-9711 (arXiv:hep-ph/9702253v1).

[8] S. K. Kang and C. S. Kim, "Majorana Neutrino Masses and Neutrino Oscillations," Phys.Rev. D63 (2001) 113010 (arXiv:hep-ph/0012046v1).

[9] Z. Z. Xing, "Vanishing Effective Mass of the Neutrinoless Double Beta Decay?" Phys.Rev. D68 (2003) 053002 (arXiv:hep-ph/0305195v2).

[10] A. Merle and W. Rodejohann, "The Elements of the Neutrino Mass Matrix: Allowed Ranges and Implications of Texture Zeros," Phys.Rev. D73 (2006) 073012 (arXiv:hep-ph/0603111v2).

[11] L. Wolfenstein, Phys. Rev. D18, 958 (1978).

[12] P. F. Harrison, D. H. Perkins and W. G. Scott, Phys. Lett. B530, 167 (2002) (arXiv:hep-ph/0202074v1) ; X. G. He and A. Zee, Phys. Lett. B560, 87 (2003) (arXiv:hep-ph/0301092v3).

[13] P. F. Harrison and W. G. Scott, "Symmetries and Generalisations of Tri-Bimaximal Neutrino Mixing," arXiv:hep-ph/0203209v2 22 Mar 2002.

[14] Z. Z. Xing, "Nearly Tri-Bimaximal Neutrino Mixing and CP Violation," Phys.Lett.B533:85-93,2002 (arXiv:hep-ph/0204049v1); A. Zee, "Parametrizing the Neutrino Mixing Matrix," Phys.Rev. D68 (2003) 093002, hep-ph/0307323v1 25 Jul 2003; A. Datta, L. Everett and P. Ramond, "Cabibbo Haze in Lepton Mixing," Phys.Lett. B620 (2005) 42-51 (arXiv:hep-ph/0503222v1); N. Li and B. Q. Ma, "Parametrization of Neutrino Mixing Matrix in Tri-Bimaximal Mixing Pattern," Phys.Rev. D71 (2005) 017302 (arXiv:hep-ph/0412126v2); J. D. Bjorken, P. F. Harrison and W. G. Scott, "Simplified Unitarity Triangles for the Lepton Sector," Phys.Rev. D74 (2006) 073012 (arXiv:hep-ph/0511201v2); S. F. King, "Parametrizing the lepton mixing matrix in terms of deviations from tri-bimaximal mixing," Phys.Lett.B659:244-251,2008 (arXiv:0710.0530v3 [hep-ph]); S. Pakvasa, W. Rodejohann and T. J. Weiler, "TriMinimal Parametrization of the Neutrino Mixing Matrix," Phys.Rev.Lett.100:111801,2008 (arXiv:0711.0052v2 [hep-ph]); C. D. Carone and R. F. Lebed, "Optimal Parametrization of Deviations from Tribimaximal Form of the Neutrino Mass Matrix," Phys.Rev.D80:117301,2009 (arXiv:0910.1529v2 [hep-ph])

[15] R. A. Porto and A. Zee, "Neutrino Mixing and the Private Higgs," Phys.Rev.D79:013003,2009 (arXiv:0807.0612v1 [hep-ph]).

[16] S. L. Glashow, "Playing with Neutrino Masses," arXiv:0912.4976v1 [hep-ph] 25 Dec 2009.

[17] C. S. Lam, "A 2-3 Symmetry in Neutrino Oscillations," Phys.Lett. B507 (2001) 214-218 (arXiv:hep-ph/0104116v1); Y. Koide, H. Nishiura, K. Matsuda, T. Kikuchi and T. Fukuyama, "Universal Texture of Quark and Lepton Mass Matrices and a Discrete Symmetry Z_3," Phys.Rev. D66 (2002) 093006 (arXiv:hep-ph/0209333v2); W. Grimus and L. Lavoura, "Maximal atmospheric neutrino mixing and the small ratio of muon to tau mass," J.Phys.G30:73-82,2004 (arXiv:hep-ph/0309050v2); C. Hagedorn and R. Ziegler, "mu-tau Symmetry and Charged Lepton Mass Hierarchy in a Supersymmetric D4 Model," SISSA 45/2010/EP (arXiv:1007.1888v1 [hep-ph]); R. N. Mohapatra and W. Rodejohann, "Broken mu-tau Symmetry and Leptonic CP Violation," Phys.Rev.D72:053001,2005 (arXiv:hep-ph/0507312v2); T. Araki and C. Q. Geng, "mu-tau symmetry in Zee-Babu model," arXiv:1006.0629v2 [hep-ph]; T. Kitabayashi and M. Yasue, "μ-τ Symmetry and Maximal CP Violation," Phys.Lett. B621 (2005) 133-138 (arXiv:hep-ph/0504212v4); R. N. Mohapatra, S. Nasri and H. B. Yu, "Grand unification of μ-τ Symmetry," Phys.Lett. B636 (2006) 114-118 (arXiv:hep-ph/0603020v1); P. F. Harrison and W. G. Scott, "Mu-Tau Reflection Symmetry in Lepton Mixing and Neutrino Oscillations," Phys.Lett. B547 (2002) 219-228 (arXiv:hep-ph/0210197v1); K. Fuki and M. Yasue, "Two Categories of

Approximately mu-tau Symmetric Neutrino Mass Textures," Nucl.Phys.B783:31-56,2007 (arXiv:hep-ph/0608042v2)

[18] P. H. Frampton, S. L. Glashow and D. Marfatia, "Zeroes of the Neutrino Mass Matrix," Phys.Lett. B536 (2002) 79-82 (arXiv:hep-ph/0201008v2)

[19] C. Jarlskog, "A Basis Independent Formulation of the Connection Between Quark Mass Matrices, CP Violation and Experiment," CERN-TH.4242/85 Aug. 1985